ELSEVIER

Journal of Photochemistry and Photobiology A: Chemistry 151 (2002) 253–265

Journal of Photochemistry and Photobiology A:Chemistry

www.elsevier.com/locate/jphotochem

Short communication

Photocatalytic oxidation of ethanol on micrometer- and nanometer-sized semiconductor particles

Bernd R. Müller[a,*], Stefan Majoni[b], Dieter Meissner[b], Rüdiger Memming[b]

[a] *Institut für Angewandte Chemie Berlin-Adlershof, e.V. (ACA), Richard-Willstätter Straße 12, 12489 Berlin, Germany*
[b] *Institut für Solarenergieforschung GmbH (ISFH), Sokelantstraße 5, 30165 Hannover, Germany*

Received 7 December 2001; accepted 9 January 2002

Abstract

The photocatalytic oxidation reaction of ethanol on small nanometer-sized and large micrometer-sized ZnS particles as well as on nanometer-sized SnO_2 under stationary illumination has been investigated in order to study the particle size effect in this size regime. It has been demonstrated that the reaction mechanism of alcohol oxidation on micrometer- and nanometer-sized particles is quite different. Ethanol is selectively oxidized on μm-ZnS to acetaldehyde without side products by a "two-hole" process. This reaction required two absorbed photons in one particle which are transferred in a very short time interval (55 ns) from the μm-ZnS particle to the ethanol molecule forming directly acetaldehyde. In the case of nm-ZnS, long-lived α-hydroxyethyl radicals are formed via a "one-hole" process due to the low generation rate of charge carriers (about $18\,e^-/h^+\,s^{-1}$) in one nm-ZnS particle. These radicals undergo secondary reactions, i.e. dimerization to 2,3-butanediol and disproportionation to acetaldehyde in the electrolyte. The electrochemical rate constant k_{et} for the slowest partial reaction occurring on the illuminated nm- and μm-ZnS particles has been calculated. One obtains similar rate constants, namely $k_{et} = 9.8 \times 10^{-9}$ and $4.3 \times 10^{-9}\,cm\,s^{-1}$ for μm-ZnS and nm-ZnS, respectively. In the case of illuminated nm-SnO_2 particles, only the oxidation product acetaldehyde was observed. Here, the initially formed α-hydroxyethyl radical via a "one-hole" process is further oxidized to the corresponding aldehyde by electron injection from the radical into the conduction band of the same SnO_2 particle by avoiding the formation of 2,3-butanediol.

Keywords: Photocatalytic oxidation; Ethanol; ZnS; SnO_2; Particle size effect

1. Introduction

Photochemical processes in heterogeneous systems have gained wide interests in recent years because of their applications in photocatalytic detoxification of polluted water [1,2] and conversion of solar energy into chemical energy [3]. On a microscopic scale, photocatalysis is a process based on the irradiation of semiconductor particles with light energy equal to or greater than its bandgap creating electrons in the conduction band and holes in the valence band. If these charge carriers are separated fast enough, they can be used for chemical reactions at the surface of the semiconductor particle [4].

In general, photocatalysis with semiconductor particles overcomes the energy barrier of a thermodynamically feasible reaction because of the excess energy stored in the photoinduced electron/hole pairs [5]. This is shown schematically in Fig. 1 for the hypothetical partial reaction of ethanol with a photoinduced hole forming in the first step a radical (intermediate) which is in principle able to react with a second hole on the surface of the semiconductor to the stable product acetaldehyde. Thus, the net reaction $CH_3CH_2OH + 2h^+ \rightarrow CH_3CH{=}O + 2H^+$ occurs in two steps and requires therefore two absorbed photons.

The reaction pathways of reactions on semiconductor surfaces in which two or more charge carriers are involved depend strongly on the time interval between the absorption of two photons incident on one particle and therefore on the particle size. Taking a suspension of about 10^8 particles (μm-diameter) in a volume of $1\,cm^3$ so that the incident light is just completely adsorbed, it takes about nanoseconds between the absorption of two photons in one particle for an incident flux of typically 10^{17} photons $cm^{-2}\,s^{-1}$. Using a colloidal solution of particles of about 3 nm size, this time

* Corresponding author. Fax: +49-30-63-22-93-20.
E-mail address: bernd.mueller@surf24.de (B.R. Müller).

1010-6030/02/$ – see front matter
PII: S1010-6030(02)00010-2

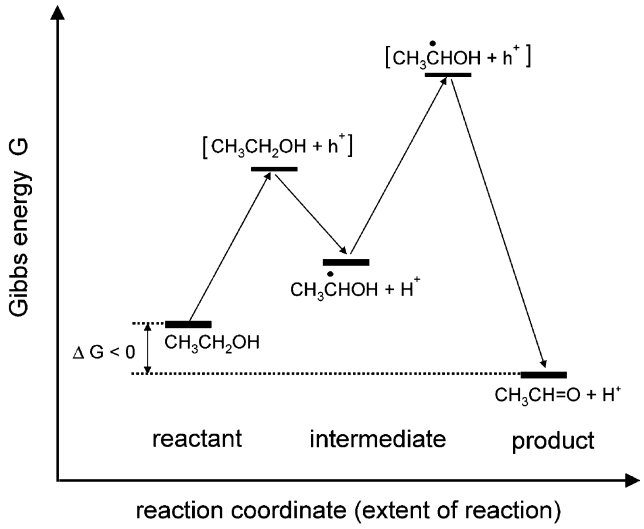

Fig. 1. Energetics of photocatalysis on illuminated semiconductor particles schematically illustrated for a chemical oxidation reaction (partial reaction) of ethanol to the α-hydroxyethyl radical (intermediate) and finally to the stable product acetaldehyde. The net reaction to acetaldehyde occurs in two steps and requires two absorbed photons.

interval is longer than six orders of magnitudes compared to the micrometer particles. This would mean that a radical formed in the first reaction step (compare Fig. 1) may undergo another reaction before a second electron or hole is available in the same particle [6].

Gerischer [5,7] analyzed theoretically the influence of the rate of oxygen reduction and the oxidative decomposition of organic molecules on different-sized TiO_2 particles and demonstrated that the kinetics of the reactions at the semiconductor/electrolyte interface, the generation rate of electron/hole pairs and the quantum yield will differ dramatically if the particle size is varied in the nanometer- to the micrometer-size regime. Beside these calculations, however, not much research has systematically been done in this field. Systematic investigations on the role of particle size have only been experimentally carried out with semiconductor particles in the nanometer-size regime, e.g. studying the photocatalytic decomposition of $CHCl_3$ on nanocrystalline TiO_2 (particle size 6–21 nm) [8], or studying the size-dependent rate of the charge transfer process from quantum-size particles (particle size 2.9–5.0 nm) to redox species in solutions [9].

In this paper, the photocatalytic oxidation reaction of ethanol on micrometer- and nanometer-sized ZnS particles as well as on nanometer-sized SnO_2 particles under stationary illumination conditions is described and discussed in terms of the decisive reaction parameters such as generation rate of charge carriers within one particle, the time interval between two successive charge transfer processes within one particle and the electrochemical rate constant for the rate-determining reaction step on the particles.

2. Experimental details

2.1. Sample preparation

All chemicals for the ZnS and SnO_2 preparation were stored under nitrogen in a glove box (MBraun, Typ 150-GI). Before use, all prepared solutions for the ZnS precipitation reactions were flushed with argon for 1 h. The purity grade of ethanol was 'for chromatography' and the water was purified by a Millipore-Q/RO system. The specific conductivity of this purified water was less than 5×10^{-8} S cm^{-1}. All other chemicals were of analytical grade and were used without further purification.

2.1.1. Preparation of micrometer-sized ZnS particles

ZnS particles with diameters in the range of micrometers have been produced by using a method described by Williams et al. [10]. Here 120 ml of a 0.88 M thioacetamide solution, 148 ml of 0.081 M $Zn(ClO_4)_2$ (Alfa Products) solution and 2 ml of concentrated H_2SO_4, all solutions being preheated to 80 °C, were mixed leading to a slow hydrolysis. Convections in the reaction solution caused by thermal gradients or stirring were avoided as good as possible. Under these conditions, the reaction forming the ZnS particles is diffusion-controlled and very uniform spherically shaped particles with an average diameter of about 4 μm were formed (derived from scanning electron microscopy (SEM) pictures). After a reaction time of 1 h, the particles were separated from the solution by centrifugation and decantation of the liquid and washed with water and finally with ammonium hydroxide to remove adsorbed H_2S. The samples were dried at 60 °C overnight under a slow nitrogen flow. According to an X-ray analysis, the μm-ZnS particles mainly consist of β-ZnS (cubic modification, 93%) with a small amount of α-ZnS (hexagonal modification, 7%). The specific surface area of the μm-ZnS particles was determined by using the BET method with a 'flow sorb' 2300 from Micromeritics. The measured surface was 20 ± 2 m^2 g^{-1}.

2.1.2. Preparation of nanometer-sized ZnS particles (colloids)

The ZnS colloids were prepared by modifying a method developed by the Henglein et al. [11]. The colloids were produced under argon by adding quickly (within about 0.5 s) 1 ml of 17 mM $Zn(ClO_4)_2$ (Alfa Product) solution to 99 ml of 0.2 mM Na_2S (purity grade p.a., Merck) solution containing water/ethanol (volume ratio: 5:1, $c_{EtOH} = 2.86$ M) and 16 mM colloidal SiO_2 (Ludox HS 40, Du Pont, particles size ≈ 15 nm) as a stabilizer. The prepared 0.17 mM ZnS colloids containing 17 mol% SH^- excess did not show any fluorescence indicating that the excess SH^- ions are specifically adsorbed on the particle surface [6]. Dunstan et al. [12] have shown from mobility measurements that all excess ions are specifically adsorbed on the ZnS surface. In order to obtain reproducible results, it was important that all

parameters in this procedure were carefully kept constant. Under these experimental conditions, an average particle size of 3.0 nm (±0.5 nm) was obtained for ZnS particles with 17 mol% SH^- excess, which was determined by transmission electron microscopy (TEM). From the bulk density of zinc sulfide (4.08 g cm^{-3}) and a molecular weight of 97.44, an average aggregation number of 357 was obtained. Photoelectrochemical measurements were always performed with particles being aged for 24 h.

2.1.3. Preparation of nanometer-sized SnO_2 particles (colloids)

The SnO_2 colloidal solution was prepared by hydrolysis of $SnCl_4$ in a modified procedure described by Mulvaney et al. [13]. A 3 ml aliquot of freshly distilled $SnCl_4$ was added dropwise under stirring to 1 l of water. The acidic solution was left standing in the dark for 24 h to allow the formation of a white amorphous precipitate. The water above the precipitate was then decanted, and the precipitate was washed with water until its pH rose to 6. Thus treated, the precipitate was then peptized by a dropwise addition of 1 M NaOH which gave rise to a clear colloidal solution of SnO_2. The solution was then subjected to dialysis against water until pH 7.5 was attained. The colloidal solutions prepared in this way, colorless and perfect clear, were found to be stable for several months. TEM revealed an average particle diameter of 2.5 nm (±0.5 nm). From the bulk density of tin dioxide (6.85 g cm^{-3}) and a molecular weight of 150.69, an average aggregation number of 224 was obtained. The pictures taken with the magnification 1:1.39 × 10^6 showed crystal planes of the individual particles which indicated that the particles were basically minute single crystals of cassiterite structure. The stability of the colloidal SnO_2 solutions in the presence of electrolyte is rather poor. In 1 M NaOH, $NaClO_4$, KCl or HCl, SnO_2 precipitates immediately after addition. We found that only $HClO_4$ was compatible with the colloid to a certain extent, depending on the concentration. In 1 M $HClO_4$, the SnO_2 solution (1 mM) was stable for several days and could be used for polarographic measurements [14].

2.2. Photoelectrochemical experiments

The photoelectrochemical (photocatalytic) investigations were carried out by using a temperature-controlled quartz vessel (volume: 95 ml) with flat windows on both sides. It was sealed with a double septum for taking gas samples and another one was taken for liquid samples by using corresponding syringes. In every experiment, the cell was filled with 70 ml suspension containing 100 mg ZnS particles (particle density: $N_{(\mu m\text{-}ZnS)} = 10.4 \times 10^6\ cm^{-3}$), or colloidal ZnS solutions ($c = 0.17$ mM), or colloidal SnO_2 solutions ($c = 6.5$ mM) and was stirred with a magnetic stirrer. Before starting the illumination, the suspension or the colloidal solution was deaerated by flushing argon through it for at least 1 h. In addition, an external argon flushing was used through the interstice of the double septum in order to avoid any penetration of oxygen through the punctured septum. All illumination experiments with micrometer- and nanometer-sized ZnS particles were carried out at pH 10 and the pH did not change during illumination in the presence of SiO_2. The cell was kept constant at a temperature of 25 °C. The irradiation was carried out by a 150 W xenon lamp (XBO 150 W/S, Osram) that was hosted in a lamp housing. The light was passed through a 10 cm thick water filter to absorb infrared light. In addition, a 280 or 320 nm cut-off filter was used. The photon intensities of the xenon lamp into the cell were measured by chemical actinometry by using iron(III) oxalate for calibration [15].

2.3. Analytic

The reaction products were mainly analyzed by gas chromatography. The gases H_2, O_2 and N_2 present in the gas phase in the quartz cell were determined by using a gas chromatograph (GC-8A, Shimadzu) at 80 °C equipped with a stainless steel column (length 2 m, diameter 4 mm) filled with a molecular sieve (0.5 nm, 60/80 mesh from Chrompack) and a heat conduction detector. The carrier gas was argon with a flow rate of 45 ml min^{-1}. The composition of the liquid was analyzed by using a gas chromatograph (HR GC 5300, Carlo Erba) which was supplied with a flame ionization detector (FID). Here we used a fused silica capillary column (DB-Wax ID 320 from J & W Scientific, AAS) with a length of 30 m and an inner diameter of 0.32 mm combined with a deactivated pre-column. Hydrogen was used as a carrier gas with a flow rate of 71 cm s^{-1}. The pressure in front of the pre-column was 60 kPa. An on-column system was used as an injection port and 5 μl of the illuminated suspension or colloidal solution was injected via the on-column system into the pre-column. In order to obtain good reproducibility in the determination of acetaldehyde and 2,3-butanediol, different temperatures were used in the detection system. In the case of 2,3-butanediol, the liquid was injected at a temperature of 100 °C and the column was then heated up to 145 °C at a rate of 15 °C min^{-1}. Under these conditions, the retention times for 2,3-butanediol were 3.51 and 3.73 min for the meso form and the racemate, respectively. For the acetaldehyde analysis, the GC was kept constant at a temperature at 50 °C. The retention time was 1.24 min.

UV–Vis spectra were recorded with the spectrometer Omega 10 (Bruins Instruments). The polarographic determination of Sn(II) ions present in the illuminated colloidal SnO_2 solution ($c = 6.5$ mM) was carried out by using the Polarecord 626 with the VA stand 663 (Metrohm) equipped with a multimode electrode, and a scanner. Here 0.5 ml of the illuminated SnO_2 solution ($c = 6.5$ mM) was diluted in 20 ml $HClO_4$. The Sn(II) ions show in 1 M $HClO_4$ a reduction potential of −0.51 V vs Ag/AgCl.

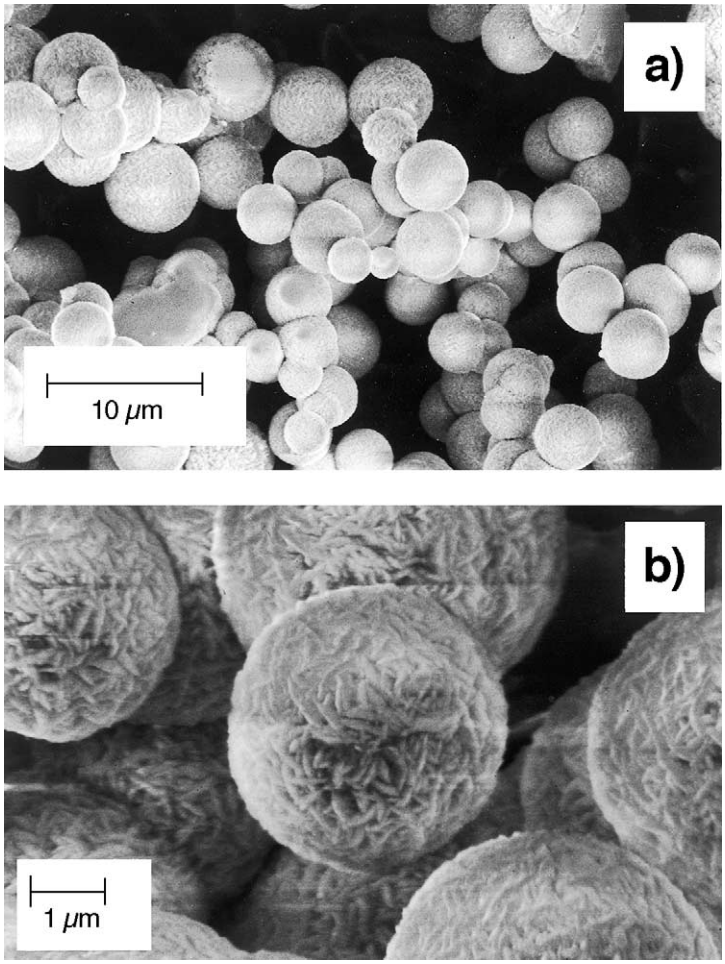

Fig. 2. (a) SEM picture of micrometer-sized ZnS particles. The growth of the particles were performed under conditions that minimize stirring and convection (see text; magnification: ×6000); (b) typical surface morphology (fibrous structure) of μm-ZnS particles (magnification: ×15 000).

3. Results

3.1. Characterization of ZnS and SnO_2 particles

Particle shape and size distribution of the micrometer-sized ZnS particles were characterized by SEM and by the BET method. Fig. 2a shows typical synthesized ZnS particles obtained after a reaction time of 60 min, and Fig. 2b illustrates the surface morphology of these particles showing a rough surface (porous surface) with a fibrous appearance, resembling needles that might have nucleated at separate sites and then grown parallel to the surface [10]. The transverse dimension of these needle-like structure is about 10–90 nm. In addition, Fig. 3 presents the size distribution diagram for the synthesized micrometer-sized ZnS particles. The ZnS particles reach an average diameter of 4.06 μm. The data of the histogram in Fig. 3 were obtained from direct measurements of the diameter of a representative group of 100 particles derived from SEM pictures. The specific surface area of the micrometer-sized ZnS particles was $20 \pm 2\,m^2\,g^{-1}$, therefore about 50 times larger than expected for particles with a smooth surface.

The nm-ZnS colloids with 17 mol% SH^- excess synthesized in the presence of the stabilizer SiO_2 were stable

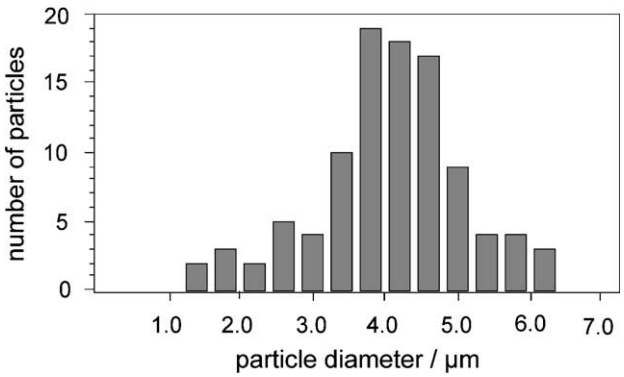

Fig. 3. Histogram of the particle size distribution for micrometer-sized ZnS particles. The data were obtained by direct measurements of 100 particles from SEM photographs. The particles reach an average diameter of 4.06 μm.

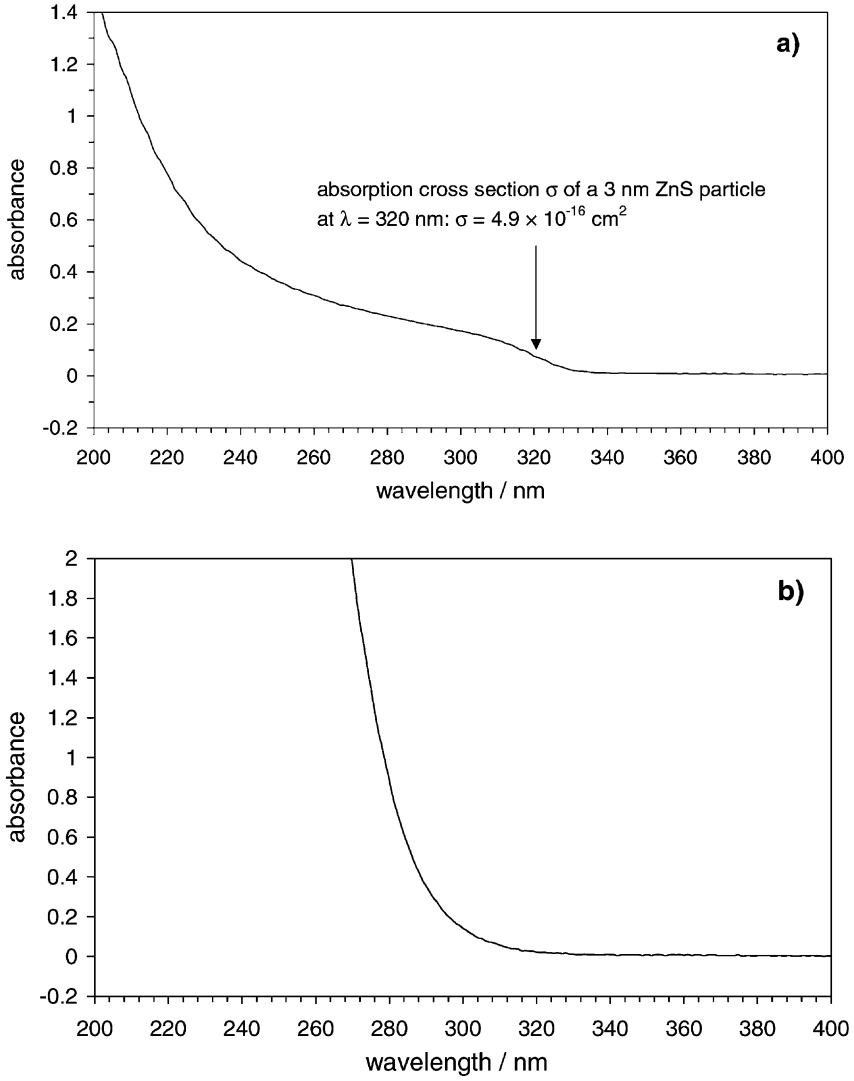

Fig. 4. (a) Absorption spectrum of a 0.17 mM ZnS sol ($N_{(\text{nm-ZnS})} = 2.86 \times 10^{14}\,\text{cm}^{-3}$) containing 17 mol% SH^- excess in water/ethanol (volume ratio 5:1) at pH 10. The ZnS colloids (average diameter 3 nm) were stabilized with 0.16 mM colloidal SiO_2. Absorption cross-section of a 3 nm-ZnS particle at $\lambda = 320\,\text{nm}$, $\sigma = 4.9 \times 10^{-16}\,\text{cm}^2$; (b) absorption spectrum of a 6.5 mM SnO_2 sol ($N_{(\text{nm-SnO}_2)} = 1.73 \times 10^{16}\,\text{cm}^{-3}$) in water/ethanol (volume ratio 5:1) at pH 7.8.

over month and their solutions were transparent. The stabilizer SiO_2 acted also as a buffer at pH 10. The average particle size of our ZnS colloids determined from the TEM micrographs was 3.0 nm (average aggregation number 357) and this is consistent with the value found in the literature [16]. The absorption spectrum of the 0.17 mM ZnS solution (containing 17 mol% SH^- excess) is shown in Fig. 4a. The colloids were aged for 24 h after synthesis and then the spectrum was recorded. The absorption starts to rise steeply at 330 nm. The onset of absorption corresponds to a bandgap of 3.76 eV which is only slightly larger than the bandgap energy of 3.70 eV of macro-crystalline ZnS [16]. The absorption cross-section for 3 nm-ZnS particles has been calculated from the measured absorbance A via

$$\sigma = \frac{2.303A}{N_{(\text{nm-ZnS})}l} \quad (1)$$

where $N_{(\text{nm-ZnS})}$ is the density of ZnS particles of the sol and l the optical path length. With $N_{(\text{nm-ZnS})} = 2.86 \times 10^{14}\,\text{cm}^{-3}$ one obtains $\sigma = 4.9 \times 10^{-16}\,\text{cm}^2$ at $\lambda = 320\,\text{nm}$. The ZnS sol with SH^- excess exhibits no fluorescence indicating that no surface recombination traps (i.e. anion vacancies [6,16]) for charge carriers within the bandgap are present.

The absorption spectrum of a 6.5 mM colloidal SnO_2 solution is shown in Fig. 4b. The onset of the absorption at about 320 nm corresponds to a bandgap of 3.88 eV which is larger than the bandgap energy of 3.50 eV of macro-crystalline SnO_2 [13]. This means that the described synthesis yields a SnO_2 colloid with a particle size small enough to result in a bandgap shift of about 0.38 eV relative to bulk SnO_2 indicating the quantum-size effect of these very small particles. The average particle size of SnO_2 was 2.5 nm (aggregation

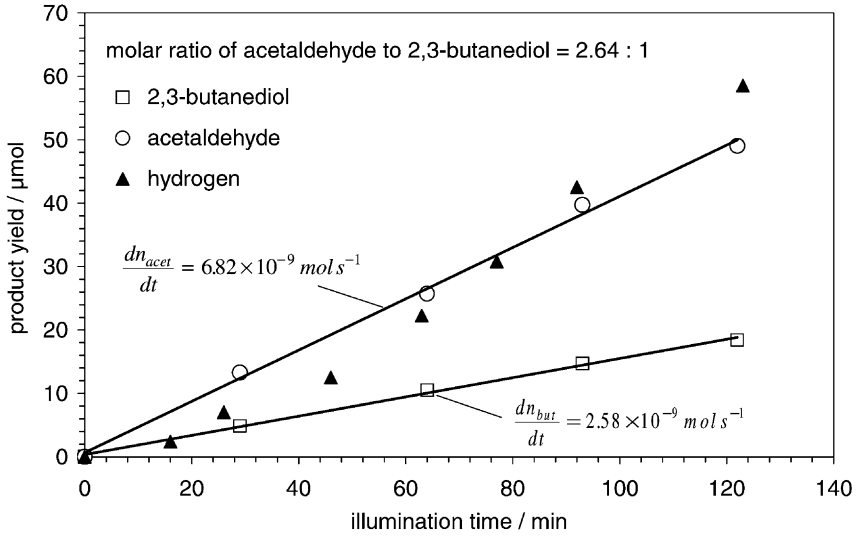

Fig. 5. Formation of hydrogen, acetaldehyde (rate, $dn_{acet}/dt = 6.82 \times 10^{-9}$ mol s^{-1}), and 2,3-butanediol (rate, $dn_{but}/dt = 2.58 \times 10^{-9}$ mol s^{-1}) on 3 nm-ZnS colloids ($c = 0.17$ mM, $N_{(nm\text{-}ZnS)} = 2.86 \times 10^{14}$ cm^{-3}) with 17 mol% SH^- excess in an ethanol/water solution (volume ratio: 1:5) at pH 10 in the presence of 16 mM colloidal SiO_2 vs illumination time; reaction volume, $V_R = 18.84$ cm^3 (see text); cut-off filter, WG 320. Molar ratio of acetaldehyde to 2,3-butanediol = 2.64:1.

number 224) derived from TEM measurements (compare Section 2).

3.2. Photoelectrochemical and photochemical experiments

Fig. 5 represents the reaction products formed during illumination ($\lambda \geq 320$ nm) of nm-ZnS colloids with an excess of 17 mol% SH^- in ethanol/water solution. Here hydrogen, acetaldehyde, and 2,3-butanediol were formed. The illumination experiment was carried out at pH 10 and the pH did not change during illumination in the presence of SiO_2 which acts as a stabilizer for the ZnS sol and also as a buffer. The amount of acetaldehyde and 2,3-butanediol increases approximately linearly with illumination time and a rate of 2.58×10^{-9} mol s^{-1} for 2,3-butanediol and 6.82×10^{-9} s^{-1} for acetaldehyde, respectively, was determined from the curves in Fig. 5. Thus, the molar ratio of acetaldehyde and 2,3-butanediol was 2.64:1 and it remained constant through the hole illumination experiment. The relative error in the measurements of the acetaldehyde and 2,3-butanediol concentration by GC was 10% and therefore the relative error of the concentration ratio was 20%. In the case of nanometer-sized ZnS particles, a 320 nm cut-off filter was used for the illumination experiments. The light source generates 1.07×10^{17} photons s^{-1} between 320 nm (cut-off filter) and 330 nm (the absorption onset of the ZnS colloids, compare Fig. 4a) on a spot of 20 mm in diameter. So we used 3.4×10^{16} photons cm^{-2} s^{-1} to excite the nm-ZnS particles (Table 1). The determination of the quantum yield for the oxidation product formed on nanometer-sized ZnS will be shown later (see Section 4).

Table 1
Comparison of decisive reaction parameters for illuminated nm- and µm-ZnS particles

	Particle diameter	
	3 nm-ZnS	4 µm-ZnS
Absorption cross-section, σ (cm^2) at 320 nm	4.9×10^{-16}	1.3×10^{-7}
Photon flux, Φ_{ph} (cm^{-2} s^{-1})	3.4×10^{16}	4.1×10^{17}
Photon flux (s^{-1})	1.07×10^{17}	1.3×10^{18}
No. of generated electron/hole pairs per particle and second, $g_{particle}$ (s^{-1})	18.0	5.3×10^{10}
Time interval between two absorptions incidences within one particle, $\Delta t = g^{-1}_{particle}$ (s)	56.0×10^{-3}	19.0×10^{-12}
Quantum efficiency (yield), Q (%)	19.6	0.034
Time interval between two successive hole transfer processes within one particle, $\Delta t_{transfer}$ (s)	306.0×10^{-3}	55.0×10^{-9}
No. of transferred holes per second across the semiconductor/electrolyte interface, $(\Delta t_{transfer})^{-1}$ (s^{-1})	3.0	18.0×10^{6}
Average lifetime of the α-hydroxyethyl radicals formed on 3 nm-ZnS (ms)	27.0	
Second-order rate constant, k^{II} (cm^3 mol^{-1} s^{-1})	734.5	3.1×10^{9}
Electrochemical rate constant, k_{et} (cm s^{-1})	4.3×10^{-9}	9.8×10^{-9}

The same type of photoreactions shown before (Fig. 5) were studied with ZnS suspensions consisting of particles with a diameter in the micrometer range. In the case of nm-ZnS particles containing 17 mol% SH^- excess the concentrations of 2,3-butanediol and acetaldehyde increase linearly with illumination time, which means that the 2,3-butanediol/acetaldehyde ratio was constant during the hole illumination experiment (Fig. 5). The illumination experiments with micrometer-sized ZnS particles were mainly performed in order to test whether different reaction products are formed at large μm-ZnS particles compared to the products formed on the nm-ZnS particles. Thus, special care was taken that the experiments were performed under the same conditions as in the case of nm-ZnS particles. In order to provide the same experimental conditions, we added SH^- ions on the order of some micromoles (7.4 μmol) to the μm-ZnS suspension. This concentration corresponds to the 17 mol% SH^- excess on 3 nm-ZnS particles mentioned above, by considering the rough surface of the micrometer particles found by BET measurements. In addition, 16 mM colloidal SiO_2 was added to the ZnS suspension in order to reach the same pH as for the colloidal ZnS solutions (pH 10). The course of the products formation during illumination of the suspension containing the μm-ZnS particles is given in Fig. 6. Here the reaction products hydrogen and acetaldehyde are formed on the illuminated ($\lambda \geq 280$ nm) micrometer-sized ZnS particles in an ethanol/water mixture. Remarkably, no 2,3-butanediol was found here. The smallest amount of 2,3-butanediol detectable according to the sensitivity of our GC was 0.5 μmol. Therefore, the ratio of acetaldehyde/2,3-butanediol here is larger than 34:1 compared with the concentration ratio of 2.64:1 found for the nm-ZnS particles with SH^- excess (Fig. 5). The total amount of formed acetaldehyde was only little less compared to the hydrogen evolution. We cannot excluded here that a small amount of hydrogen was dissolved in the suspension and cannot be detected in the gas phase (see Section 2). The amount of acetaldehyde increases approximately linearly with illumination time and a rate of 0.363×10^{-9} mol s^{-1} acetaldehyde was determined from the curve in Fig. 6. For the illumination experiments with 4 μm-ZnS particles a 280 nm cut-off filter was used. The photon flux to excite the micrometer particles here was 1.3×10^{18} photons s^{-1} which are completely absorbed from the suspension. From the photon flux and the rate of acetaldehyde formation, a quantum yield of 0.034% can be calculated assuming that two holes were consumed for the ethanol oxidation process (Table 1).

After the illumination experiments, the nm- and μm-ZnS particles were proven by adding methylviologen (colorless MV^{2+}) to the suspension or colloidal solution. However, no Zn^0 was found after illumination on the particles. In order to check whether this negative result, very small amount of Zn^0 was added to the illuminated suspension or colloidal solution after this test with viologen. After addition of Zn^0 the blue color of the $MV^{\bullet+}$ radical appears within some seconds. This means that no zinc metal was deposited on the nanometer- and micrometer-sized ZnS particles with SH^- excess after illumination.

Fig. 7 illustrates the reaction products formed during illumination ($\lambda \geq 280$ nm) on 6.5 mM colloidal SnO_2 dispersed in ethanol/water. A small amount of hydrogen (1.48 μmol) was observed in the gas phase after a illumination time of 238 min. In addition, the colloidal SnO_2 particles were reduced to Sn(II) during illumination. After 245 min, 9.28 μmol Sn(II) was formed on the colloids. This means that about 2% of the Sn(IV) ions (455 μmol Sn(IV) in 70 cm^3 colloidal solution) of SnO_2 was reduced to Sn(II). The observed yellow color of the SnO_2 sol after illumination

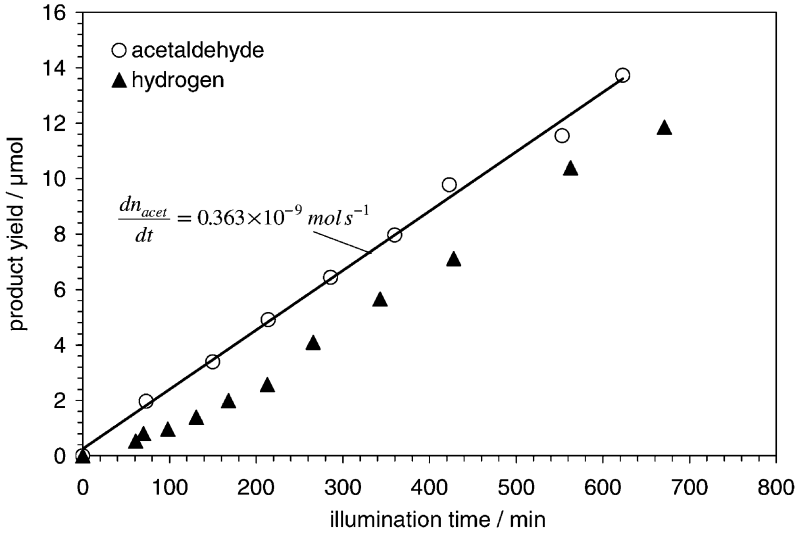

Fig. 6. Formation of hydrogen and acetaldehyde (rate, 0.363×10^{-9} mol s^{-1}) on 4 μm-ZnS particles ($N_{(\mu m\text{-}ZnS)} = 10.4 \times 10^6\ cm^{-3}$) in an ethanol/water solution (volume ratio 1:5) at pH 10 vs illumination time. No 2,3-butanediol has been detected in the suspension. The suspension contains 7.4 μmol of SH^- ions and 16 mM SiO_2; reaction volume, $V_R = 2.40\ cm^3$ (see text); cut-off filter, WG 280; quantum yield 0.034% (acetaldehyde formation).

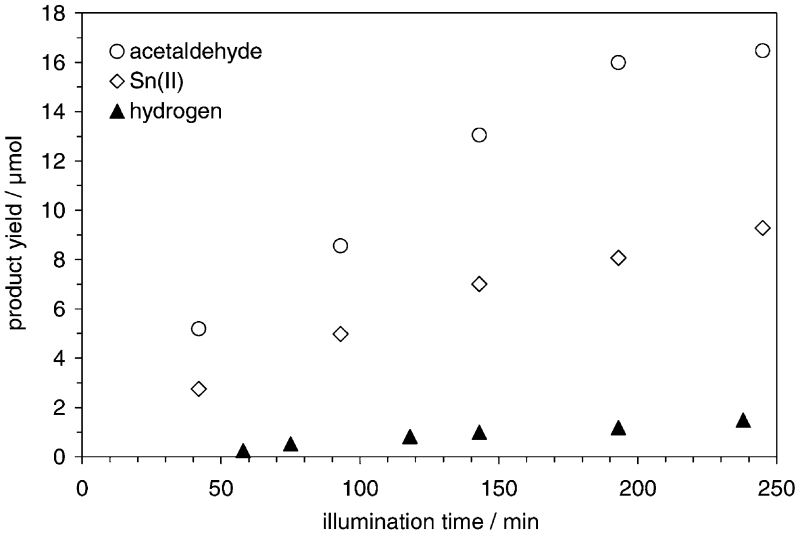

Fig. 7. Formation of hydrogen, acetaldehyde and tin(II) on a 6.5 mM SnO_2 sol ($N_{(nm\text{-}SnO_2)} = 1.73 \times 10^{16}\,cm^{-3}$; average particle diameter 2.5 nm) in an ethanol/water solution (volume ratio 1:5) vs illumination time. No 2,3-butanediol has been detected in the colloidal solution; cut-off filter, WG 280; during illumination the pH changes from 7.8 to 8.2.

indicates also the formation of Sn(0), but this photoinduced metal deposition on the colloids here was not investigated in more detail. After 245 min, 16.47 μmol acetaldehyde was formed on nm-SnO_2. The product 2,3-butanediol was not detected in the colloidal SnO_2 solution (detection limit: 0.5 μmol) after illumination. Therefore, the ratio of acetaldehyde/2,3-butanediol here is larger than 33:1. During illumination the pH of the colloidal solution changes slightly from pH 7.8 to 8.2.

Since ZnS and SnO_2 colloids absorb light only in the UV region because of their large bandgap (3.76 eV for ZnS and 3.88 eV for SnO_2; compare Fig. 4), we also checked whether any photochemical reactions already occur without the semiconductor but with molecules formed on this. A well-known photoreaction is the formation of 2,3-butanediol upon excitation of acetaldehyde in ethanol solution as given by [17]

$$CH_3CH{=}O + CH_3CH_2OH + h\nu \rightarrow H_3CCH(OH)CH(OH)CH_3 \quad (2)$$

Since this reaction occurs at a high quantum yield, we illuminated a solution (free from ZnS) containing a relatively large acetaldehyde concentration (11.3 mM) in ethanol by using a 280 nm cut-off filter. Indeed, we then found considerable concentration of 2,3-butanediol. If instead a lower acetaldehyde concentration of 0.3 mM is used (this corresponds to the amount of acetaldehyde formed on the nm-ZnS colloids after a 100 min illumination) by using a 320 nm cut-off filter (Fig. 5), then no 2,3-butanediol could be detected even after a 1 h illumination by using a 280 nm cut-off filter. This result is due to the low extinction coefficient ($\varepsilon = 3.98\,M^{-1}\,cm^{-1}$) of acetaldehyde at $\lambda_{max} = 280$ nm. Hydrogen was not found in these photochemical reactions. Thus, acetaldehyde formed on the ZnS colloids does not photochemically react in a detectable amount to 2,3-butanediol under our illumination conditions. This photochemical reaction (photoreduction [17]) can be neglected here and the formation of 2,3-butanediol is exclusively contributed to the photoinduced reactions occurring on the nm-ZnS particles with SH^- excess (compare Fig. 5).

4. Discussion

4.1. Oxidation of ethanol on micrometer-sized ZnS particles

As already mentioned in Section 1 ethanol is expected to be oxidized at illuminated semiconductor particles by a transfer of two holes being created successively by light absorption within the particle according to the following reactions:

$$CH_3CH_2OH + h_{(VB)}{}^+ \rightarrow CH_3CHOH + H^+ \quad (3a)$$

$$CH_3CHOH + h_{(VB)}{}^+ \rightarrow CH_3CH{=}O + H^+ \quad (3b)$$

where VB is the valence band.

The reaction of ethanol with a valence band hole forming the α-hydroxyethyl radical in the first step according to Eq. (3a) and forming finally acetaldehyde in a second step (Eq. (3b)) at one particle without side reaction can only occur if the time interval $\Delta t_{transfer}$ between two successive hole transfer processes on one particle is sufficiently short and the residence time of the initially formed α-hydroxyethyl radical on/or near the surface of the particle is longer than $\Delta t_{transfer}$ (compare Eq. (6)). Under our illumination conditions, the time interval between two absorption incidences

within one micrometer-sized particle is about 19 ps (see Table 1 and discussion below), and considering the relative low quantum yield of 0.034% for the formation of acetaldehyde the time interval between two successive hole transfer processes is about 55 ns (see Table 1 and Eq. (6)). During this time the initially formed α-hydroxyethyl radical could in principle diffuse about $l = 18$ nm calculated from the equation $l = (6D\,\Delta t_{\text{transfer}})^{0.5}$ with $D = 10^{-5}\,\text{cm}^2\,\text{s}^{-1}$. Thereby this diffusion length of the α-hydroxyethyl radical is smaller than the needles (dimension about 10–90 nm) which are forming the rough surface of the particles (see the fibrous surface of the μm-ZnS particles in Fig. 2b). Therefore, we assume that the time interval of about 55 ns is too short for the initially formed radical (Eq. (3a)) to diffuse from the porous surface into the electrolyte. Therefore, the radical is further oxidized by a second hole according to Eq. (3b) to form acetaldehyde. We call this oxidation process a two-hole process. The reaction scheme for the two-hole process, the energy scheme illustrating the valence and conduction band of macroscopic ZnS and the redox potentials for the oxidation processes are illustrated in Fig. 8.

To determine the generation rate g_{particle} of electron/hole pairs in one semiconductor particle, one has to calculate at first the absorption cross-section for photons. Gerischer and Heller [18] have calculated this cross-section for spherical micrometer-sized semiconductor particles whose sizes are larger than the threshold wavelength λ_g of the semiconductor applying geometrical optics. They obtained [18]

$$\sigma \approx \pi R^2[1 - \exp(-\alpha 2R)] \tag{4}$$

where R is the particle radius and α the absorption coefficient of the semiconductor. Macroscopic ZnS has a bandgap of 3.70 eV [19] and therefore absorbs light below $\lambda_g = 0.34\,\mu\text{m}$. This value is much smaller than the particle radius and Eq. (4) can be applied for calculation. With $\alpha = 3.7 \times 10^4\,\text{cm}^{-1}$, as typical value for a direct bandgap semiconductor [6], a cross-section of $\sigma = 1.3 \times 10^{-7}\,\text{cm}^2$ is derived for one ZnS particle with a diameter of 4.06 μm (Table 1). The generation rate g_{particle} of electron/hole pairs in one particle can be calculated according to the following equation:

$$g_{\text{particle}} = \sigma \Phi_{\text{ph}} \tag{5}$$

With a photon flux of $\Phi_{\text{ph}} = 4.1 \times 10^{17}\,\text{photons}\,\text{cm}^{-2}\,\text{s}^{-1}$, the generation rate g_{particle} is $5.3 \times 10^{10}\,\text{e}^-/\text{h}^+$ pairs per particle and second (Table 1), whereby scattering of light on the micrometer particles has been neglected. This means that the time interval between two absorptions incidences within one 4 μm-ZnS particle is 19 ps (g^{-1}_{particle}). The time interval between two successive hole transfer processes can be expressed considering the generation rate g_{particle} and the quantum yield Q with respect to the acetaldehyde formation

$$\Delta t_{\text{transfer}} = (Q g_{\text{particle}})^{-1} \tag{6}$$

With $Q = 0.034\%$ and the generation rate calculated above, one obtains $\Delta t_{\text{transfer}} = 55$ ns for our large micrometer-sized ZnS particles (see also the discussion above, and Table 1). This means that 18×10^6 holes ($\Delta t^{-1}_{\text{transfer}}$) per second are transferred across the semi-conductor/electrolyte interface to oxidize ethanol (Table 1).

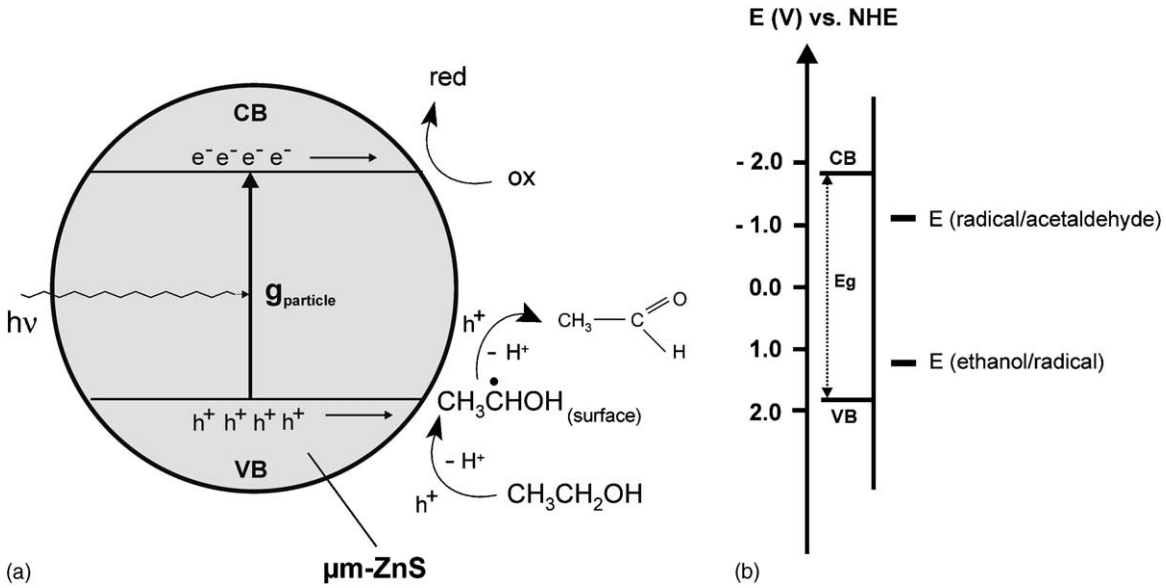

Fig. 8. (a) Proposed reaction mechanism (two-hole process) of the ethanol oxidation on illuminated 4 μm-ZnS particles. The two-hole process required two absorbed photons in one μm-ZnS particle which are transferred in a very short time interval ($\Delta t_{\text{transfer}} = 55$ ns) from the particle to the ethanol molecule forming directly acetaldehyde; g_{particle}, generation rate of charge carriers in one μm-ZnS particle ($g_{\text{particle}} = 5.3 \times 10^{10}\,\text{s}^{-1}$, see Table 1); (b) energy scheme of ZnS particles and redox potentials of the ethanol/α-hydroxyethyl radical, and α-hydroxyethyl radical/acetaldehyde system at pH 10 (from Ref. [6]); CB, conduction band; VB, valence band; E_g, bandgap.

In the case of illuminated semiconductor particles, the slowest partial reaction determines the overall reaction rate under open circuit conditions. In our system, the ethanol oxidation process (anodic reaction) or the reduction of water to hydrogen in alkaline (pH 10) solution (cathodic reaction: $2H_2O + 2e_{CB}^- \rightarrow H_2 + 2OH^-$) on ZnS is responsible for the overall reaction rate. In general, we assumed that the reaction between the illuminated 4 μm-ZnS particles and the ethanol molecule is a bimolecular reaction. Under this assumption, the formation of acetaldehyde can be described by the following kinetics:

$$\frac{1}{V_R}\frac{dn_{acet}}{dt} = k^{II} c_{EtOH} c_{T(\mu m\text{-}ZnS)} \quad (7)$$

where c_{EtOH} is the concentration of ethanol, $c_{T(\mu m\text{-}ZnS)}$ the ZnS particle concentration of the ZnS suspension ($c_{T(\mu m\text{-}ZnS)} = N_{(\mu m\text{-}ZnS)}/N_L$), N_L is the Avogadro number), k^{II} the second-order rate constant and V_R the reaction volume where the formation of acetaldehyde on the illuminated ZnS occurs. The light in the reaction cell was completely absorbed by about 25×10^6 μm-sized ZnS particles. With the particle density of $N_{(\mu m\text{-}ZnS)} = 10.4 \times 10^6\,cm^{-3}$ the reaction volume is $2.40\,cm^{-3}$. With $dn_{acet}/dt = 0.363 \times 10^{-9}\,mol\,s^{-1}$ (compare Fig. 6), $V_R = 2.40\,cm^3$, $c_{EtOH} = 2.86\,mmol\,cm^{-3}$, $c_{(\mu m\text{-}ZnS)} = 17.3 \times 10^{-18}\,mol\,cm^{-3}$ one obtains $k^{II} = 3.1 \times 10^9\,cm^3\,s^{-1}\,mol^{-1}$ (Table 1). In an analysis of the transport (diffusion) of the redox species from the bulk to the surface of the particles and the kinetics of the charge transfer process across the semiconductor/electrolyte interface at a spherical micro-electrode, several workers [19–24] have shown that the second-order rate constant k^{II} (units in $cm^3\,mol^{-1}\,s^{-1}$) can be related to the electrochemical rate constant k_{et} (units in $cm\,s^{-1}$) according to the following equation:

$$\frac{1}{k^{II}} = \frac{1}{4\pi R^2 N_L}\left[\frac{1}{k_{et}} + \frac{R}{D}\right] \quad (8)$$

where D is the diffusion coefficient of the redox species, R the particle radius and N_L the Avogadro number. According to Eq. (8) with $D = 1.0 \times 10^{-5}\,cm^2\,s^{-1}$ for ethanol [25] and $k^{II} = 3.1 \times 10^9\,cm^3\,s^{-1}\,mol^{-1}$ (see Table 1), an electrochemical rate constant of $9.8 \times 10^{-9}\,cm\,s^{-1}$ is derived for the rate-determining reaction on the illuminated 4.06 μm-ZnS particles (Table 1). This means that the rate-determining reaction on the particle is not diffusion-controlled because in this case the maximal electrochemical rate constant $k_{et,\,diff}$ would be six orders of magnitudes higher ($k_{et,\,diff} = D/R = 0.049\,cm\,s^{-1}$ [26]).

The reactions of photoinduced charge carriers in semiconductor particles after generation are very complex. They can recombine by band-to-band and/or via bulk or surface states located energetically in the bandgap [27]. All recombination processes reduce the density of charge carriers at the interface. The very low observed quantum yield (0.034% for the formation of acetaldehyde) indicates that the main part of the generated charge carriers recombines and only a very small fraction reacts with ethanol and water forming acetaldehyde and hydrogen. From our experiments, we have not enough information about the recombination processes occurring on the μm-ZnS particles. But it is possible that the rough surface of the synthesized μm-ZnS particles (determined by SEM and BET measurements) is responsible for the low quantum yield because this surface can act as a recombination center for the photoinduced charge carriers. Further investigations must therefore be performed in future by using different-sized μm-ZnS particles with different surface morphologies.

4.2. Oxidation of ethanol at nanometer-sized ZnS particles

The absorption cross-section σ for photons for a 3 nm-ZnS particle has been calculated according to Eq. (1). One obtains a cross-section of $\sigma = 4.9 \times 10^{-16}\,cm^2$ at a wavelength of $\lambda = 320\,nm$ (see Table 1 and Fig. 4a). With a photon flux of $\Phi_{ph} = 3.4 \times 10^{16}\,photons\,cm^{-2}\,s^{-1}$ (Table 1), the generation rate $g_{particle}$ of electron/hole pairs in one 3 nm-ZnS particle is only $18\,e^-/h^+\,s^{-1}$ (compare Eq. (5) and the data obtained with micrometer-sized particles, Table 1). The corresponding time interval between two absorption incidences ($\Delta t = g_{particle}^{-1}$) within one 3 nm-ZnS particle is therefore about 56 ms. Thus, it is in principle possible that the initially formed α-hydroxyethyl radical formed by a one-hole process on the 3 nm-ZnS particle diffuses from the particle surface to undergo subsequent reactions such as dimerization and disproportionation to form stable products (2,3-butanediol according to Eq. (9a), and acetaldehyde according to Eq. (9b)) as given by

$$2CH_3CHOH \rightarrow H_3CCH(OH)CH(OH)CH_3 \quad (9a)$$

$$2CH_3CHOH \rightarrow CH_3CH_2OH + CH_3CH{=}O \quad (9b)$$

In principle, the secondary reactions of radicals can occur either on the surface of the particle or in the bulk of the electrolyte. We assume that the latter process is dominant on nm-ZnS particles with SH^- excess for two reasons:

(a) The ratio of formed acetaldehyde to 2,3-butanediol found in our illumination experiments with ZnS colloids is about 2.64 (see Fig. 5), which is close to the ratio found for the well-investigated free α-hydroxyisopropyl radicals in solution [28]. This radical reacts completely analogous to our system, forming acetone and pinacol in a ratio of $\gamma = 3.4$. This slightly larger value for this radical is probably due to the higher steric hindrance for the dimerization reaction in the case of the very bulky α-hydroxyisopropyl radical compared to the α-hydroxyethyl radical.

(b) The ratio 2.64:1 is constant throughout the hole illumination experiment as it is typical for reactions of free radicals in homogeneous solution. On the other hand, if the secondary reaction of the radicals would occur on

the surface of the particles, γ would probably increase above 2.6 because the probability for a direct second oxidation step would also increase when the radical concentration rises with time on the surface [6].

Independent of all assumptions concerning the reaction sites, it is clear from our experiments that only in the case of small nm-ZnS particles 2,3-butanediol is formed (Fig. 5) whereas in the case of large μm-ZnS particles this product is missing (Fig. 6).

Applying the reactions as given by Eqs. (9a) and (9b) and using the experimental data on the formation of butanediol ($dn_{but}/dt = 2.58 \times 10^{-9}$ mol s^{-1}, Fig. 5) in a bimolecular (second-order) reaction of two radicals, one can determine the average lifetime of the free hydroxyethyl radicals in solution. From the kinetics and the generation rate of the α-hydroxyethyl radicals g_{rad} on the illuminated nm-ZnS particles and the dimerization/disproportionation reactions in the electrolyte (compare Eqs. (9a) and (9b)), one can calculate the stationary radical concentration c_{rad} in the electrolyte as given by

$$c_{rad} = \sqrt{\frac{g_{rad}}{2(k_{disp} + k_{dim})}} \tag{10}$$

in which the generation rate of radicals g_{rad} is given by

$$\frac{1}{V_R}\frac{dn_{rad}}{dt} = g_{rad} = 2\left[g_{but}\left(\frac{k_{disp}}{k_{dim}} + 1\right)\right] \tag{11}$$

with $g_{but} = (1/V_R \times dn_{but}/dt)$ being the generation rate of butanediol (units in mol l^{-1} s^{-1}). From the results given in Fig. 5, the term n_{but}/dt is 2.58×10^{-9} mol s^{-1}. With $V_R = 18.84$ cm^3 (reaction volume in the ZnS sol: $V_R = L_{cell} \times A_{beam} = 6.0$ cm $\times$ 3.14 cm^2), $g_{but} = 1.37 \times 10^{-7}$ mol l^{-1} s^{-1}. With the ratio $\gamma = k_{disp}/k_{dim} = 2.64$ one obtains from Eq. (11) $g_{rad} = 1.0 \times 10^{-6}$ mol l^{-1} s^{-1}. According to Eq. (10) and with $2(k_{disp} + k_{dim}) = 1.4 \times 10^9$ mol l^{-1} s^{-1} [28], the stationary radical concentration in the electrolyte is $c_{rad} = 2.67 \times 10^{-8}$ mol l^{-1}. From these data, the average lifetime of the free radicals in the solution is then given by

$$\tau = \frac{1}{2(k_{disp} + k_{dim})c_{rad}} \tag{12}$$

Using the above-calculated data one obtains $\tau = 27$ ms (Table 1). This time is much shorter than the time interval of two successive charge transfer processes in a single 3 nm-ZnS particle which is about 300 ms (Table 1 and see discussion below).

Based on the reaction mechanism summarized in Fig. 9, the quantum yield Q with respect to the formation of the α-hydroxyethyl radicals on nm-ZnS can be calculated by considering the generation rate dn_{rad}/dt of the radicals (units in mol s^{-1}) according to the following equation:

$$\frac{dn_{rad}}{dt} = 2\left[\frac{dn_{but}}{dt}\left(\frac{k_{disp}}{k_{dim}} + 1\right)\right] \tag{13}$$

With $k_{disp}/k_{dim} = 2.64$ and $dn_{but}/dt = 2.58 \times 10^{-9}$ mol s^{-1} (compare Fig. 5), one obtains $dn_{rad}/dt = 18.8 \times 10^{-9}$ mol s^{-1}. The illuminated ZnS sol in the quartz cell

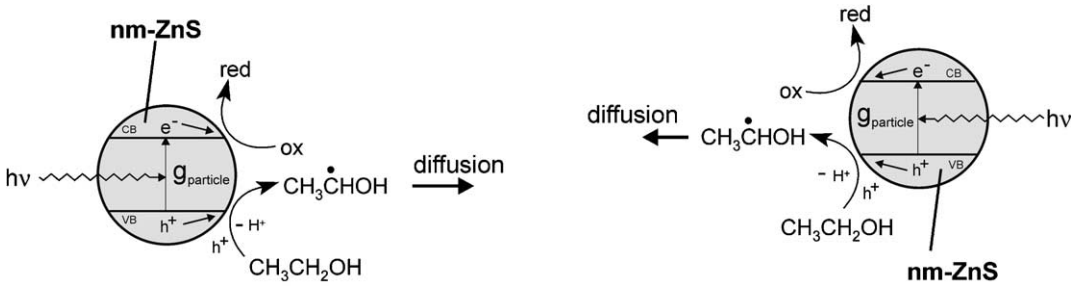

reactions of free radicals in the bulk of the electrolyte

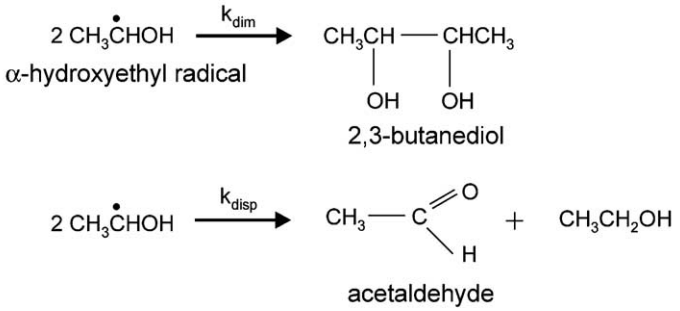

Fig. 9. (a) Proposed reaction mechanism (one-hole process) of the ethanol oxidation on illuminated 3 nm-ZnS particles to α-hydroxyethyl radicals and the subsequent reactions of the radicals in the bulk of the electrolyte to 2,3-butanediol (dimerization reaction, k_{dim}) and acetaldehyde (disproportionation reaction, k_{disp}); $k_{disp}/k_{dim} = 2.64$; $g_{particle}$, generation rate of charge carriers in one 3 nm-ZnS particle ($g_{particle} = 18$ s^{-1}, see Table 1).

absorbs a fraction of about 54% of the photons generated by the light source between 320 nm (cut-off filter) and 330 nm (the absorption onset of the ZnS colloids, Fig. 4a). With 1.07×10^{17} photons s^{-1} (Table 1), 96×10^{-9} mol photons s^{-1} ($0.54 \times 1.07 \times 10^{17}\,s^{-1}/N_L$) were absorbed by the ZnS sol between 320 and 330 nm. Thus, the quantum yield with respect to the α-hydroxyethyl radical formation on nm-ZnS is 19.6% (Table 1). From this result, the time interval between two successive hole transfer processes in one nm-ZnS particle, $\Delta t_{transfer}$, can be expressed according to Eqs. (5) and (6) ($\Delta t_{transfer} = Q\sigma\Phi_{ph})^{-1}$, and one obtains for $\Delta t_{transfer} = 306$ ms. This time is about one order of magnitude longer than the average lifetime τ of the α-hydroxyethyl radicals ($\tau = 27$ ms, Table 1) formed on nm-ZnS by a one-hole process.

If we assume that the reaction of ethanol with the illuminated 3 nm-ZnS particle to the α-hydroxyethyl radical by a one-hole is a bimolecular reaction, the second-order rate constant k^{II} can be calculated according to the following equation:

$$\frac{1}{V_R}\frac{dn_{rad}}{dt} = k^{II} c_{EtOH} c_{T(nm\text{-}ZnS)} \quad (14)$$

With $c_{EtOH} = 2.86 \times 10^{-3}$ mol cm^{-3}, $c_{T(nm\text{-}ZnS)} = 2.86 \times 10^{14}\,cm^{-3}/N_L = 4.75 \times 10^{-10}$ mol cm^{-3}, $V_R = 18.84\,cm^3$ (reaction volume in the ZnS sol) and $dn_{rad}/dt = 18.8\times10^{-9}$ mol s^{-1}, one obtains $k^{II} = 734.5\,cm^3\,s^{-1}\,mol^{-1}$ (Table 1). This value is about six orders of magnitudes lower than the second-order rate constant k^{II} calculated for the micrometer-sized ZnS particles (compare Table 1). With $k^{II} = 734.5\,cm^3\,s^{-1}\,mol^{-1}$ and $R = 1.5 \times 10^{-7}$ cm s^{-1}, an electrochemical rate constant of 4.3×10^{-9} cm s^{-1} has been calculated according to Eq. (8) for the rate-determining reaction occurring on the illuminated 3 nm-ZnS particles (Table 1). Remarkable that the values of the electrochemical rate constants k_{et} for the μm-ZnS and for the nm-ZnS particle are of the same order of magnitude and k_{et} is therefore not size-dependent although the mechanism of alcohol oxidation is quite different on micrometer- and nm-ZnS particles (compare Figs. 8 and 9). Thus, this indicates that the reduction process (hydrogen formation) is probably the rate-determining step on the nanometer- and micrometer-sized ZnS particles.

Based on the generation rate of α-hydroxyethyl radicals ($dn_{rad}/dt = 18.8 \times 10^{-9}$ mol s^{-1}) on illuminated nm-ZnS, an amount of 69.4 μmol (138.74/2 μmol) hydrogen after an illumination time of 123 min has been expected by considering the charge balance of electrons and holes generated by light in the same nm-ZnS particles ($dn_{hydrogen}/dt = \frac{1}{2}\,dn_{rad}/dt$). Fig. 5 shows that after 123 min illumination, only 58.5 μmol hydrogen was detected. The analytical determination of hydrogen was only carried out in the gas phase, but not in the colloidal solution (see Section 2). Therefore we cannot exclude here that hydrogen was dissolved in the solution and/or was adsorbed on the surface of the nm-ZnS particles to a certain extent (compare Fig. 6; the detected amount of hydrogen formed on micrometer-sized ZnS was also little less compared to the amount of acetaldehyde).

4.3. Oxidation of ethanol on nanometer-sized SnO_2 particles

In the case of nm-ZnS particles with 17 mol% SH^- excess, the formation of acetaldehyde and 2,3-butanediol was observed during illumination (Fig. 5). In contrast to these results, only acetaldehyde as an oxidation product was observed in the case of illuminated nanometer SnO_2 particles. The reaction product 2,3-butanediol was not found in the colloidal SnO_2 solution after illumination. In addition, the illuminated SnO_2 colloids were partly reduced to Sn(II). These results can be explained by the following reaction sequence:

$$CH_3CH_2OH + h_{(VB)}{}^+ \rightarrow CH_3CHOH + H^+ \quad (15a)$$

$$2CH_3CHOH + [SnO_2] \rightarrow [SnO_2(2e_{(CB)}{}^-)] + 2H^+ + 2CH_3CH{=}O \quad (15b)$$

$$[SnO_2(2e_{(CB)}{}^-)] \rightarrow [SnO_2(Sn^{2+})] \quad (15c)$$

In the first step, the ethanol molecule is oxidized on illuminated SnO_2 to the α-hydroxyethyl radical by a one-hole process according to Eq. (15a). This radical is an electron-transfer agent with a strong reducing power (−1.10 V vs NHE at pH 10 [6], see energy scheme in Fig. 8) and, i.e. electron transfer to colloidal TiO_2 [29], WO_3 [30] and ZnO [31,32] has been observed because in these metal oxide semiconductors (including SnO_2 [13]) the lower edge of the conduction band is positioned close to 0 V vs NHE [33]. Thus, it is possible that the α-hydroxyethyl radicals inject immediately after generation an electron into the conduction band of the SnO_2 colloid forming acetaldehyde as the oxidation product (current doubling effect [34]), which would almost explain the absence of 2,3-butanediol in this experiment (compare the energy scheme in Fig. 8). The electrons stored in the conduction band (Eq. (15b)) may be used for the reduction of the Sn(IV) ions of the SnO_2 colloid to Sn(II) according to Eq. (15c) because the overall reduction of SnO_2, i.e. to $Sn(OH)_2$ may thermodynamically be possible (+0.075 V vs NHE [35]). In fact, the formation of Sn(II) shows that SnO_2 was cathodically reduced by electrons during illumination. The reduction of Pb(IV) to Pb(II) in PbO_2 colloids has also been observed if the colloids were attacked by strong reducing radicals such as CH_2OH [36].

5. Conclusions

The very different generation rates of electron/hole pairs in nanometer and micrometer-sized ZnS particles as well as the different positions of the conduction bands located energetically at the semiconductor/electrolyte interface of ZnS and SnO_2 lead to different reaction mechanisms for

the light-induced oxidation of ethanol. To the best of our knowledge, it is the first time that this phenomenon has been studied systematically on semiconductor particles in the nanometer- to micrometer-size regime. It is concluded that on ZnS and on SnO_2 radicals are formed in a primary photoinduced oxidation step via a one-hole process. The secondary reactions of these intermediates now depend, on the one hand, strongly on the position of the lower edge of the conduction band located energetically at semiconductor/electrolyte interface and, on the other hand, on the availability of a second hole generated by light in the same particle. In the case of defect free nm-ZnS particles (showing no fluorescence via surface states located energetically in the bandgap), it takes more than 50 ms before the next photon is absorbed by the same particle and even about 300 ms before the next successful charge transfer process occurs on this particle. If the radicals cannot inject electrons into the conduction band of the semiconductor (this was found for ZnS with a conduction band located energetically at high position), the radicals have plenty of time to diffuse into the electrolyte where disproportionation and dimerization of radicals can take place. If the lower edge of the conduction band of the semiconductor is energetically positioned below the redox potential of the radical, these radicals are able to inject electrons into the conduction band of the semiconductor. This is fulfilled in the case of nanometer SnO_2 particles because here the radical is further oxidized to the corresponding aldehyde by electron injection into the conduction band of the same SnO_2 particle.

On μm-ZnS the formation of long-lived radicals plays a much less important role and the oxidation of ethanol can proceed here via a two-hole process without forming dimerization products. We cannot exclude that the very porous surface of the self-synthesized μm-ZnS particle also supports the two-hole process, because the initially produced short-lived radical may here be trapped within the pores leading to a second oxidation step. In order to investigate this in more detail, particles with a different surface morphology, including such with a smooth surface, should be studied.

The values of the electrochemical rate constants for the μm-ZnS ($k_{et} = 9.8 \times 10^{-9}\,cm\,s^{-1}$) and for the nm-ZnS particle ($k_{et} = 4.3 \times 10^{-9}\,cm\,s^{-1}$) are of the same order of magnitude. This means that velocity of the rate-determining step on the ZnS particles depends not significantly on the particle size.

Acknowledgements

We thank Dr. R. Hiesgen (ISFH) for supporting SEM, and Dr. Vogel and Dr. M. Giersig (HMI, Berlin) for supporting TEM investigations. Financial support by the German Ministry of Education and Research (BMBF) under contract 0329580 and by the Deutsche Forschungsgemeinschaft (DFG) under contract Ma 1902 is gratefully acknowledged.

References

[1] E. Pelizzetti, C. Minero, Electrochim. Acta 38 (1993) 47.
[2] M.R. Hoffmann, S.T. Martin, W. Choi, D.W. Bahnemann, Chem. Rev. 95 (1995) 69.
[3] K.I. Zamaraev, V.N. Parmon, Catal. Rev. 22 (1980) 261.
[4] N. Serpone, Sol. Energy Mater. Sol. Cells 38 (1995) 369.
[5] H. Gerischer, Electrochim. Acta 38 (1993) 3.
[6] B.R. Müller, S. Majoni, R. Memming, D. Meissner, J. Phys. Chem. B 101 (1997) 2501.
[7] H. Gerischer, A. Heller, J. Phys. Chem. 95 (1991) 5261.
[8] Z. Zhang, C.-C. Wang, R. Zakaria, J.Y. Ying, J. Phys. Chem. B 102 (1998) 10871.
[9] H. Matsumoto, H. Uchida, T. Matsunaga, K. Tanaka, T. Sakata, H. Mori, H. Yoneyama, J. Phys. Chem. 98 (1994) 11549.
[10] R. Williams, P.N. Yocom, F.S. Stofko, J. Colloid Interf. Sci. 106 (1985) 388.
[11] A. Henglein, M. Gutierrez, Ch. Fischer, Ber. Bunsenges. Phys. Chem. 88 (1984) 170.
[12] D.E. Dunstan, A. Hagfeldt, M. Almgren, H.O.G. Siegbahn, E. Mukhtar, J. Phys. Chem. 94 (1990) 6797.
[13] P. Mulvaney, F. Grieser, D. Meisel, Langmuir 6 (1990) 567.
[14] M. Heyrovsky, J. Jirkovsky, B.R. Müller, Langmuir 11 (1995) 4239.
[15] C.G. Hatchard, C.A. Parker, Proc. R. Soc. A 253 (1956) 518.
[16] A. Henglein, M. Gutierrez, Ber. Bunsenges. Phys. Chem. 87 (1983) 852.
[17] N.J. Turro, Modern Molecular Photochemistry, University Science Book, Mill Valley, CA, 1991, p. 381.
[18] H. Gerischer, A. Heller, J. Electrochem. Soc. 139 (1992) 113.
[19] F.-R.F. Fan, P. Leempoel, A.J. Bard, J. Electrochem. Soc. 130 (1983) 1866.
[20] W.J. Albery, P.N. Bartlett, J. Electroanal. Chem. 131 (1982) 17.
[21] M. Grätzel, A.J. Frank, J. Phys. Chem. 86 (1982) 2964.
[22] G.T. Brown, J.R. Darwent, P.D.I. Fletcher, J. Am. Chem. Soc. 107 (1985) 6446.
[23] A. Mills, P. Douglas, G. Williams, J. Photochem. Photobiol. A 48 (1989) 397.
[24] J. Moser, M. Grätzel, J. Am. Chem. Soc. 105 (1983) 657.
[25] R. Brdicka, Grundlagen der Physikalischen Chemie, VEB Verlag, Berlin, 1976, p. 342.
[26] A.J. Bard, L.R. Faulkner, Electrochemical Methods, Wiley, New York, 1980, p. 145.
[27] K. Misawa, H. Yao, T. Hayashi, T. Kobayashi, Chem. Phys. Lett. 183 (1991) 113.
[28] A. Henne, H. Fischer, Helv. Chim. Acta 58 (1975) 1598.
[29] A. Henglein, Ber. Bunsenges. Phys. Chem. 87 (1983) 474.
[30] M.T. Nenadovic, T. Rajh, O.I. Micic, A. Nozik, J. Phys. Chem. 88 (1984) 5827.
[31] U. Koch, A. Fojtik, H. Weller, A. Henglein, Chem. Phys. Lett. 122 (1985) 507.
[32] D.W. Bahnemann, C. Kormann, M.R. Hoffmann, J. Phys. Chem. 91 (1987) 3789.
[33] R. Memming, Prog. Surf. Sci. 17 (1984) 7.
[34] S. Yamagata, S. Nakabayashi, K.M. Sancier, A. Fujishima, Bull. Chem. Soc. Jpn. 61 (1988) 3429.
[35] A. Bard, R. Parsons, J. Jordan (Eds.), Standard Electrode Potentials in Aqueous Solution, Marcel Decker, New York, 1985.
[36] A. Kumar, A. Henglein, H. Weller, J. Phys. Chem. 93 (1989) 2262.